J Mater Sci (2006) 41:4744–4748
DOI 10.1007/s10853-006-0035-6

Photophysical properties of Eu^{3+} and Tb^{3+}-doped $ZnAl_2O_4$ phosphors obtained by combustion reaction

B. S. Barros · P. S. Melo · R. H. G. A. Kiminami · A. C. F. M. Costa · G. F. de Sá · S. Alves Jr

Received: 4 May 2005 / Accepted: 23 September 2005 / Published online: 4 May 2006

Abstract Europium- and terbium-doped zinc aluminate oxide nanocrystals with a spinel structure were successfully prepared by a combustion method, using urea as fuel. The samples thus obtained were characterized by X-ray diffraction, scanning electron microscopy and luminescence spectroscopy. X-ray diffraction results confirmed the formation of $ZnAl_2O_4$ spinel phase and a minor amount of ZnO. Our SEM results revealed agglomerates in the shape of irregular plates composed of nanoparticles with dispersed points of second phase in the surface. Powders containing Eu^{3+} and Tb^{3+} ions displayed red and green photoluminescence, respectively.

Introduction

Semiconductor nanocrystals doped with rare earth ions have been investigated exhaustively in recent years. These materials show interesting enhanced optical properties, with potential applications in the design of optoelectronic materials and as efficient phosphor materials for flat-panel displays [1]. The development of advanced flat panel displays and lighting technology such as field-emission displays (FEDs) and plasma panels (PDPs) requires phosphor, which is highly efficient at low excitation voltages, highly resistant to current saturation, possesses high chemical and thermal stability, and a longer lifetime at high current densities [2–4].

Metal oxide phosphors have attracted much attention for field emission display (FED) and plasma display panel (PDP) applications because these materials are much more chemically stable than conventional sulfide phosphors such as ZnS:Cu, Al, Mn; Y_2O_2S:Eu, Tb and LaO_2S:Eu,Tb [5–7]. The excitation mechanism in FEDs is cathodoluminescent, while in PDPs it is photoluminescent, as in EL devices, which are solid-state analogs to cathodoluminescent vacuum tubes (CRT) [7].

Zinc aluminate ($ZnAl_2O_4$) belongs to a class of inorganic materials called spinels. This material has a close-packed face-centered cubic structure with Fd3m space group symmetry [8]. The optical band gap of polycrystalline $ZnAl_2O_4$ semiconductors is 3.8 V [9], which indicates that zinc aluminate in the polycrystalline form is transparent for light. This material possesses wavelengths of up to 320 nm, making it useful in ultraviolet photoelectronic devices [10] and attracting considerable interest among researchers for a variety of applications. For example, it is being studied as a candidate material for reflective optical coatings in aerospace applications [11], as a phosphor material [12] and as an ultraviolet transport electroconductive oxide [13]. Zinc aluminate doped with rare earth metal ions has been investigated most frequently because of the unique luminescent properties resulting from its stability and high emission quantum yields [12, 14, 15]. This material produces efficient visible emissions in a 4f shell, which is, to a large extent, insensitive to the influence of its surroundings thanks to

B. S. Barros · P. S. Melo · A. C. F. M. Costa
Department of Materials Engineering, Federal University of Campina Grande, Campina Grande, PB, Brazil

G. F. de Sá · S. Alves Jr
Rare Earth Laboratory – BSTR, Department of Fundamental Chemistry, Federal University of Pernambuco, Recife, PE, Brazil

R. H. G. A. Kiminami (✉)
Department of Materials Engineering, Federal University of São Carlos, São Carlos, SP, Brazil
e-mail: ruth@power.ufscar.br

the shielding effect of the outer 5s and 5p orbitals [16]. Rare earth-activated phosphors can be prepared by a variety of techniques, e.g., the hydrothermal method [12], spray pyrolysis [15], Pechini's method [5] and combustion synthesis [17].

Among the aforementioned chemical synthesization methods, combustion reaction synthesis stands out as a promising alternative method for obtaining nanosize afterceramic phosphors. This experimental approach, also known as auto-propagating synthesis, allows one to obtain particles (without pre-sintering) with sizes of about 30 nm [18]. Compared with other synthesization methods, the combustion reaction process offers the advantages of being fast and simple, without requiring subsequent intermediary calcinations stages, apart from consuming less energy during synthesis [15]. Moreover, the non-conventional combustion reaction method synthesizes highly pure, chemically homogeneous powders, usually resulting in products possessing the desired structures and composition due to their high homogeneity aided by the salts' water solubility, allowing nanosize particles to be obtained.

This paper reports on the use of combustion reaction synthesis to produce a new class of phosphor powder-based zinc aluminate spinels doped with Eu^{3+} and Tb^{3+} ions.

Experimental

Powder phosphors of $ZnAl_2O_4$:TR, where TR = Eu^{3+} and Tb^{3+}, were prepared by combustion reaction. Combustion reaction synthesis involves mixing metallic ions (nitrates, acetates or oxides) acting as oxidizing reagents with a filler that acts as the reducing agent. This redox mixture consisted of zinc nitrate—$Zn(NO_3)_2{\cdot}6H_2O$, aluminum nitrate—$Al(NO_3)_3{\cdot}9H_2O$, europium oxide—Eu_2O_3, terbium oxide—Tb_2O_3 and urea—$CO(NH_2)_2$. The proportion of each reagent was defined according to its respective molar amounts. Stoichiometric compositions of metal nitrates and rare oxide as urea were calculated based on the components' total oxidizing and reducing coefficients for the stoichiometric balance, so that the equivalence ratio (Φ_c) was unity and the energy released was maximum [18]. Carbon, hydrogen, zinc, aluminum, europium and terbium were considered reducing elements whose respective valences were +4, +1, +2, +3, +3 and +3. The oxygen was considered an oxidizing agent with a valence of −2. The valence considered for nitrogen was 0. The solutions were prepared by mixing them in a Pyrex beaker and heating them directly on a hot plate at 480 °C until self-ignition occurred.

The powder sample phases were identified by X-ray diffractometry (XRD-6000 Shimadzu, Cu Kα radiation, 40 KV and 30 mA). The scanning speed per step was 0.02^{o} and 1 s in the 2θ range of 10°–80°. The morphological characteristics of the powders obtained by combustion reaction were analyzed by scanning electron microscopy (Philips/XL30—FEG)—SEM. Photoluminescence emission (PL) and excitation (PLE) measurements were taken using a K2 Multifrequency Phase Fluorimeter.

Results and discussion

Figure 1 shows the X-ray patterns of pure $ZnAl_2O_4$ powder and powder doped with rare earth ions (Eu^{3+}, Tb^{3+}). The X-ray patterns confirmed that the samples prepared by combustion reaction consisted of single phase $ZnAl_2O_4$ spinel. The presence of secondary phase ZnO was confirmed in the sample doped with Eu^{3+} and Tb^{3+}. The formation of the secondary ZnO phase was attributed to the formation of vacancies resulting from the incorporation of rare earth ions into the host lattice. The nature of the Eu^{3+} and Tb^{3+} ions doping the nanoparticle $ZnAl_2O_4$ spinels appears to be complex, for it is possible that these ions substitute the trivalent Al^{3+} ions or divalent Zn^{2+} ions [11, 17]. Due to their large ionic radius, the Eu^{3+} (0.95 Å) and Tb^{3+} (1.0 Å) ions prefer sites with high coordination numbers (six or higher) [18]. In the $ZnAl_2O_4$ spinel structure, octahedral sites having the coordination number six are originally occupied by trivalent ions Al^{3+} (0.53 Å).

Table 1 shows the calculated lattice parameters, crystallite size and degree of crystallinity of the powders. The lattice parameters resulting from these patterns for cubic spinel phase in the powders were calculated using the program PowderX [19] and are in good agreement with the

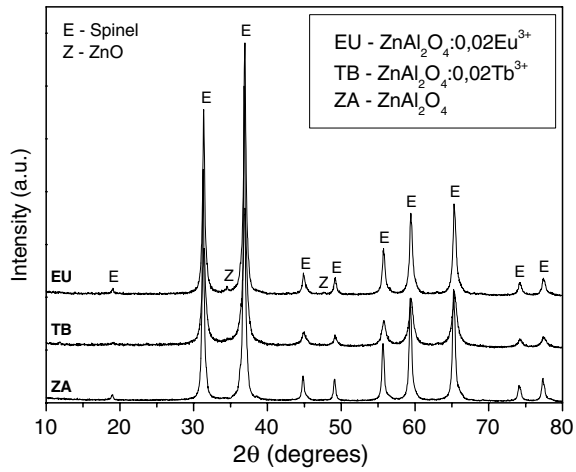

Fig. 1 X-ray diffraction patterns of pure and rare earth-doped $ZnAl_2O_4$ powders obtained by combustions reaction

Table 1 Lattice parameters, crystallite size and degree of crystallization of the powders obtained by combustion reaction

Sample	Degree of crystallinity (%)	Crystallite size (nm)	Lattice parameter (Å)
$ZnAl_2O_4$	73.9	27.1	$a = b = c = 8.0875$
$ZnAl_2O_4:Eu^{3+}$	65.5	23.6	$a = b = c = 8.0877$
$ZnAl_2O_4:Tb^{3+}$	54.1	14.4	$a = b = c = 8.0865$

reported values ($a = b = c = 8.088$/JCPDS #82-1043). The crystallinity of the powders obtained by combustion reaction was measured from the integrated area of the diffraction peak, using Shimadzu's Crystallinity software. This crystallinity decreased with the incorporation of the rare earth ions because of the high disorder these ions produce in the lattice host in response to the ionic radius mismatch between rare earth ions and Zn^{2+} or Al^{3+} ions. The average crystallite size was calculated from X-ray line broadening (d_{311}) using Scherrer's equation [20]. All the samples presented crystallite sizes of less than 30 nm.

The morphological aspect of the resulting powders was examined by scanning electronic microscopy (SEM), as shown in Fig. 2. The micrographs reveal the formation of soft agglomerates (sizes of around 5 and 40 μm) composed of nanometric scale particles. These agglomerates display an irregular morphology in the form of plates. An X-ray diffraction indicated that most of these agglomerates consisted of $ZnAl_2O_4$. The surface of the $ZnAl_2O_4$ phase showed small agglomerates and secondary phase ZnO particles.

Figure 3 depicts the excitation spectra for the $ZnAl_2O_4$ powders doped, respectively, with Eu^{3+} and Tb^{3+}. An examination of the excitation spectrum of the europium-doped sample (Fig. 3a) reveals a broad band centered on 265 nm. According to García-Hipólito et al. [21], this band originates from charge transfer transitions from O^{-2} to Eu^{+3} ions. The charge transfer state is usually the most intense excitement mechanism, generally occurring between 250 nm and 300 nm. Other excitement peaks, visible between 350 nm and 425 nm, correspond to transitions to $^7F_0$ to $^5D_4$ (373 nm) $^5L_6$ (396 nm) and $^5D_3$ (416 nm), respectively. The excitation spectrum of $ZnAl_2O_4:Tb^{3+}$ (Fig. 2b) displays a broad band centered at 232 nm. This band was attributed to the $4f^8 \rightarrow 4f^85d^1$

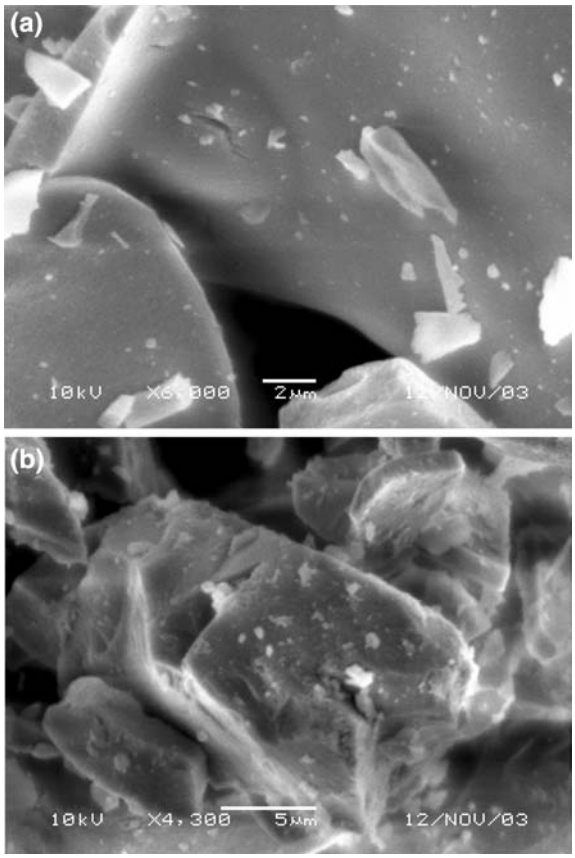

Fig. 2 SEM micrographs showing the morphology of rare earth-doped $ZnAl_2O_4$ powders obtained by combustions reaction:(**a**) Eu^{3+}, 6000×; and (**b**) Tb^{3+}, 4300×

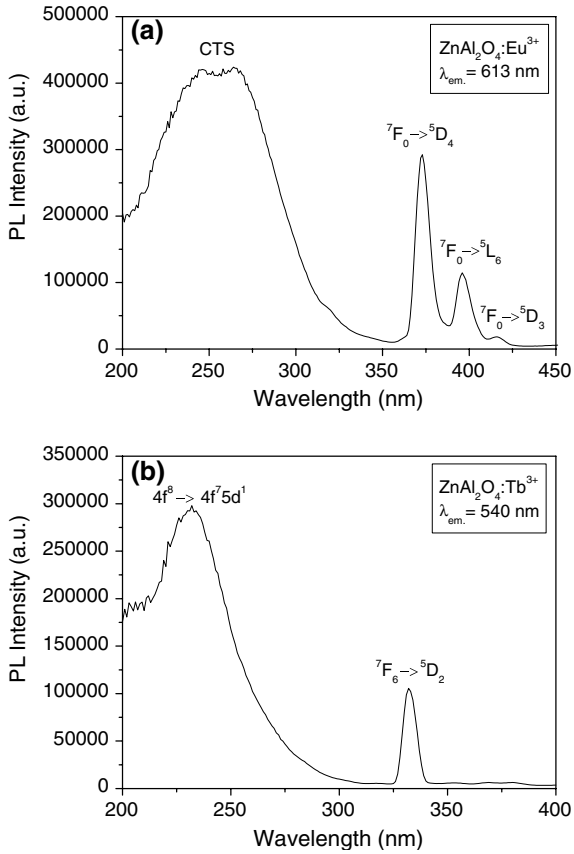

Fig. 3 Excitation spectra of $ZnAl_2O_4$ powders doped with: (**a**) $0.02Eu^{3+}$ and (**b**) $0.02Tb^{3+}$

transition (f → d transition) of Tb^{3+} and a peak centered at 332 nm corresponds to the $^7F_6 \rightarrow {}^5D_2$ transition.

Figure 4 shows the emission spectra of the powders, with the typical red photoluminescence (PL) from Eu^{3+} ions in the Eu^{3+}-doped $ZnAl_2O_4$ powder depicted in Fig. 4a. The luminescence spectrum of this ion is slightly influenced by surrounding ligands of the host material, because electronic transitions of Eu^{3+} involve only a redistribution of electrons within the inner 4f sub-shell [11]. The most intense emission peak, centered at 613 nm, corresponds to the $^5D_0 \rightarrow {}^7F_2$ transition, which takes place through the forced electric dipole (FED). This peak, which is more intense than the one centered at 591 nm, corresponds to the $^5D_0 \rightarrow {}^7F_1$ transition and occurs by means of the magnetic dipole (MD), indicating that the ion Eu^{3+} is in a low symmetry environment [22]. Other peaks, which are visible at 578, 653 and 703 nm, correspond to transitions from the $^5D_0$ to the $^7F_0$, $^7F_3$ and $^7F_4$ levels, respectively. Fig. 4b shows the major green emission peak at 543 nm and few minor peaks at 489, 586 and 622 nm in the Tb^{3+}-doped sample. These peaks represent the $^5D_4 \rightarrow {}^7F_5$, $^5D_4 \rightarrow {}^7F_6$, $^5D_4 \rightarrow {}^7F_4$ and $^5D_4 \rightarrow {}^7F_3$ transitions, respectively [8, 11]. The emission spectra of both samples also show emission peaks between 420 nm and 490 nm, generated by the lattice host $ZnAl_2O_4$.

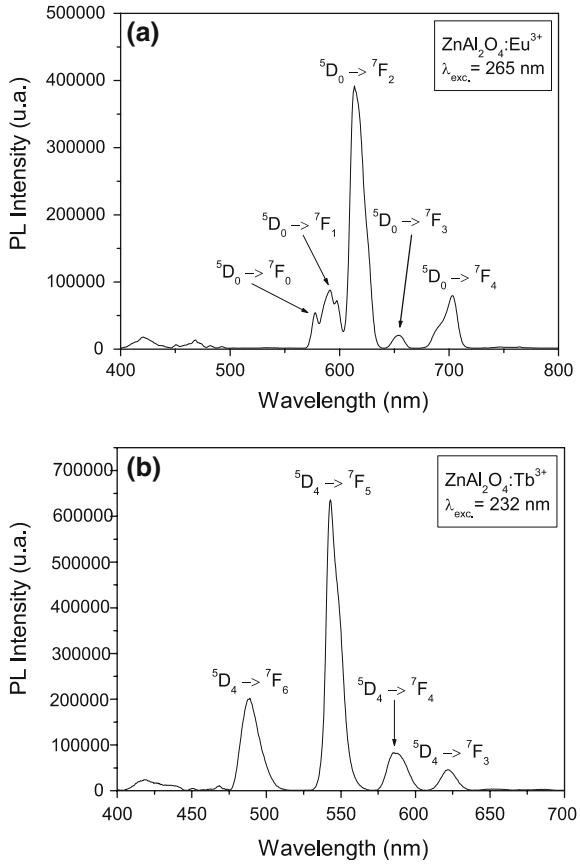

Fig. 4 Emission spectra of $ZnAl_2O_4$ powders doped, with (**a**) $0.02Eu^{3+}$ and (**b**) $0.02Tb^{3+}$

Conclusions

Nanocrystalline zinc aluminate spinels doped with europium and terbium ions were prepared by combustion synthesis. The formation of the spinel phase was confirmed by X-ray diffraction data, which were also used to calculate the lattice parameters of this phase. Our results demonstrated that no significant alteration occurred in comparison with data reported in the literature, indicating that only a minor portion of the rare earth ions may have been effectively incorporated into the host lattice, with the remainder likely adsorbed on the surface of the particles owing to the spinel's porosity.

Characteristic red and green luminescence from Eu^{3+} and Tb^{3+} ions was observed in each phosphor. The luminescence emission of europium-doped $ZnAl_2O_4$ powders was characteristic of Eu^{3+} ions. The hypersensitive forced electric-dipole emission ($^5D_0 \rightarrow {}^7F_2$) was dominant and is a property required for display applications. Characteristic emission lines of Tb^{3+} ions were also identified. The luminescent properties of Eu (III) and Tb (III), allied with the intrinsic photochemical proprieties of $ZnAl_2O_4$, make the compounds produced here possible sources of new photoelectronic devices.

Acknowledgements The authors would like to thank the Brazilian institutions CAPES and RENAMI-CNPq for their financial support of this research.

References

1. Strek W, Deren P, Bednarkiewicz A, Zawadaski M, Wrzyszcz J (2000) J Alloys Comp 300–301:456
2. Blasse G (1994) Luminescent Materials. Springer, New York
3. Yen WM, Shionoya S (eds) (1998) Phosphor Handbook. CRC press, Boca Raton, FL
4. Lou Z, Hao J (2004) Thin Solid Films 450:334
5. Xu Z, Li Y, Liu Z, Xiong Z (2004) Mater Sci Eng B 110:3002
6. Bang J, Abloudi M, Abrams B, Holloway PH (2004) J Lumin 106:171
7. Leskela M (1998) J Alloys Comp 275–277:702
8. Hill RJ, Craig JR, Gibbs GV (1979) Phys Chem Minerals 4:317
9. Sampath SK, Cordor JF (1998) J Am Ceram Soc 81:649
10. Mathur S, Veth M, Mass M, Shem H, Lecerf N, Huch V, Aufier S, Haberkorn R, Beck HP, Jilab M (2001) J Am Ceram Soc 84:1921
11. Sampath SK, Kanhere DG, Randey R (1999) J Phys Condens Matter 11:3635
12. Zawadzki M, Wrzyszcz J, Strek W, Hreniak D (2001) J Alloys Compounds 323–324:279
13. Omata T, Veda N, Veda K (1994) Appl Phys Lett 64:1077
14. Gu F, Wang SF, Lu MK, Qi YX, Zhou GJ, Xu D, Yuan DR (2004) Optical Mater 25:59

15. Lou Z, Hao J (2004) Thin Solid Films 450:334
16. Dieke GH (1968) In: Crosswhite HM and Crosswhite H (ed) Spectra and Energy Levels of Rare Earth Ions in Crystals, Interscience Publishers, New York
17. Barros BS, Costa ACFM, Kiminami RHAG, Gama L (2004) J. Metastable Nanocryst Mater 20–21:325
18. Jain SR, Adiga KC, Vernek VP (1981) Combustión Flame 40:71
19. Dong C (1997) Powder-X Report. Institute of Physics, Chinese Academy of Sciences, Beijing
20. Klung H, Alexander L (1962) In X-ray diffraction procedures. Willey, New York, EUA, p 491
21. García-Hipólito M, Hernández-Pérez CD, Alvarez-Fregoso O, Martínez E, Guzmán-Mendoza J, Falcony C (2003) Optical Materials 22:345
22. Silva JEC (1997) Geração e controle das cores-luz primárias em materiais vítreos dopados com tríades de lantanídeos. Recife, Programa de Pós-Graduação em Ciências, UFPE, Dissertação de mestrado